NASA TECHNICAL MEMORANDUM

NASA TM X-1565

NASA TM X-1565

PRELIMINARY MEASURED AND PREDICTED XB-70 ENGINE NOISE

by Paul L. Lasagna and Norman J. McLeod

Flight Research Center
Edwards, Calif.

NATIONAL AERONAUTICS AND SPACE ADMINISTRATION • WASHINGTON, D. C. • APRIL 1968

NASA TM X-1565

PRELIMINARY MEASURED AND PREDICTED XB-70 ENGINE NOISE

By Paul L. Lasagna and Norman J. McLeod

Flight Research Center
Edwards, Calif.

NATIONAL AERONAUTICS AND SPACE ADMINISTRATION

For sale by the Clearinghouse for Federal Scientific and Technical Information
Springfield, Virginia 22151 – CFSTI price $3.00

PRELIMINARY MEASURED AND PREDICTED XB-70 ENGINE NOISE

By Paul L. Lasagna and Norman J. McLeod
Flight Research Center

SUMMARY

Noise measurements on the ground were made during takeoffs, a landing, and a flyby of the XB-70 airplane. Noise predictions made by using the SAE method differed from the measured levels. The substitution of standard-day atmosphere for actual atmosphere improved the comparison of the measured and predicted noise spectra. Further investigation is needed to determine the reasons for the differences between the measured and the predicted levels. Perceived noise levels of the XB-70 were approximately 7 PNdB to 10 PNdB higher than the maximum overall sound-pressure levels in decibels.

INTRODUCTION

The continued increase in airplane engine size and thrust requires the investigation of noise from aircraft that utilize such engines. Measured noise levels are converted to perceived noise levels (ref. 1) and used by some airports to determine airplane acceptability in nearby communities. Although methods are available for predicting noise levels for new-generation aircraft, it still remains to verify the predictions and to further investigate, in detail, noise from high-thrust engines.

This paper presents measured and predicted noise levels and computed perceived noise levels for the XB-70 airplane during takeoffs, a landing, and a flyby at Edwards Air Force Base, Calif. The SAE jet-noise prediction method (ref. 2) was used to predict noise levels for comparison with measured values.

NOISE PREDICTIONS

Method

The SAE method for predicting the overall sound-pressure level (OASPL) for one engine was modified by the addition of 5 log 6 to obtain the OASPL for the six engines of the XB-70 on the ground and the addition of 10 log 6 to obtain the in-flight predicted levels. The SAE method uses separate curves, based upon Strouhal number, to predict the noise spectra on the ground and in flight. The difference in sound levels and the shift in frequency spectrum between ground predictions and flight predictions is attributed to ground reflection, interference of terrain, and airplane velocity.

Predictions in this paper are for a standard day unless otherwise stated. The acoustic standard day has a temperature of 59° F (288° K) and a relative humidity of 70 percent. The method for applying atmospheric acoustic absorption values for other than a standard day is discussed in references 2 and 3. Actual-day atmospheric acoustic absorption values would lower the predicted sound levels in the 1000, 2000, 4000, and 8000 hertz octave bands, since the actual relative humidity (table I) was much lower than that for a standard day. No effective sound reduction would occur in the frequency bands below 1000 hertz.

Errors

The effect on the predicted noise levels of errors in the measurement of engine parameters is analyzed in the appendix. For one engine the maximum variation of the predicted noise level is from 1 dB for significant engine operating parameters in error by 1 percent to 10 dB for significant operating parameters in error by 10 percent. Previous work indicated that the engine thrust calculations made by using the gas-generator method averaged 2 percent higher than test-cell values for military power, with a standard deviation equivalent to ±2 percent of the thrust. This standard deviation would indicate a possible average error of 2 dB in the predicted overall noise levels for a single engine. For six engines the possible error is approximately 5 dB when a root-mean-square analysis is used.

The effect of engine clustering on the accuracy of the predicted noise level is unknown.

INSTRUMENTATION

Noise-Measurement Range

The NASA Flight Research Center, at Edwards, Calif., has developed and is operating a noise-measurement range (ref. 4). The range is along and beyond the 300-foot-wide, 15,000-foot-long (91.4-meter-wide, 4572-meter-long) main runway at Edwards Air Force Base, as shown in figure 1. Twelve separate, self-contained microphone stations and a signal conditioning and recording system comprise the noise-measurement range.

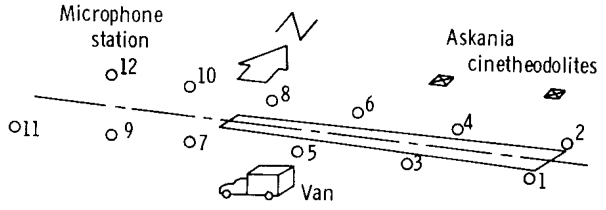

Microphone station	Distance from -			
	East end of runway,		Centerline of runway,	
	ft	m	ft	m
1, 2	0	0	155	47
3, 4	4,700	1,433	220	67
5, 6	9,700	2,957	290	88
7, 8	14,800	4,511	360	110
9, 10	19,700	6,005	430	131
11, 12	24,800	7,559	500	152

Figure 1.— Layout of the NASA noise-measurement range along the main runway at Edwards Air Force Base, Calif.

A schematic diagram of a microphone station and the signal conditioning and recording system is shown in figure 2. A photograph of a typical microphone station is shown in figure 3. The station consists of a microphone, tripod, and a standard Bruel and Kjaer (B and K) type 2801 microphone power supply with an

amplifier to drive the data signal through buried cable to an instrument van. Power is supplied by batteries and an inverter.

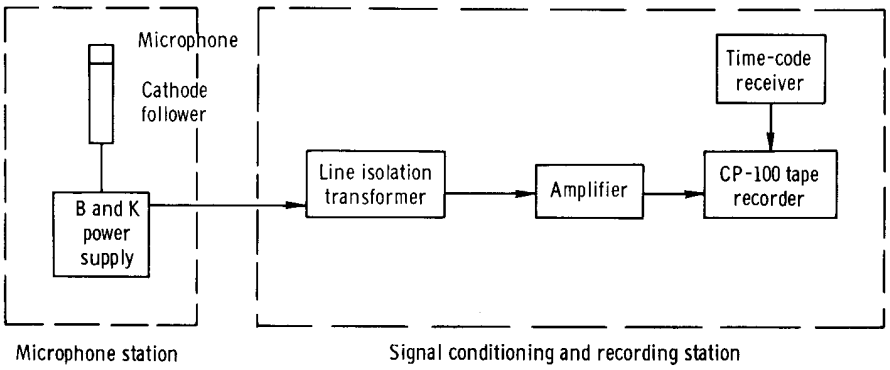

Figure 2.– Schematic diagram of a microphone station and the signal conditioning and recording station.

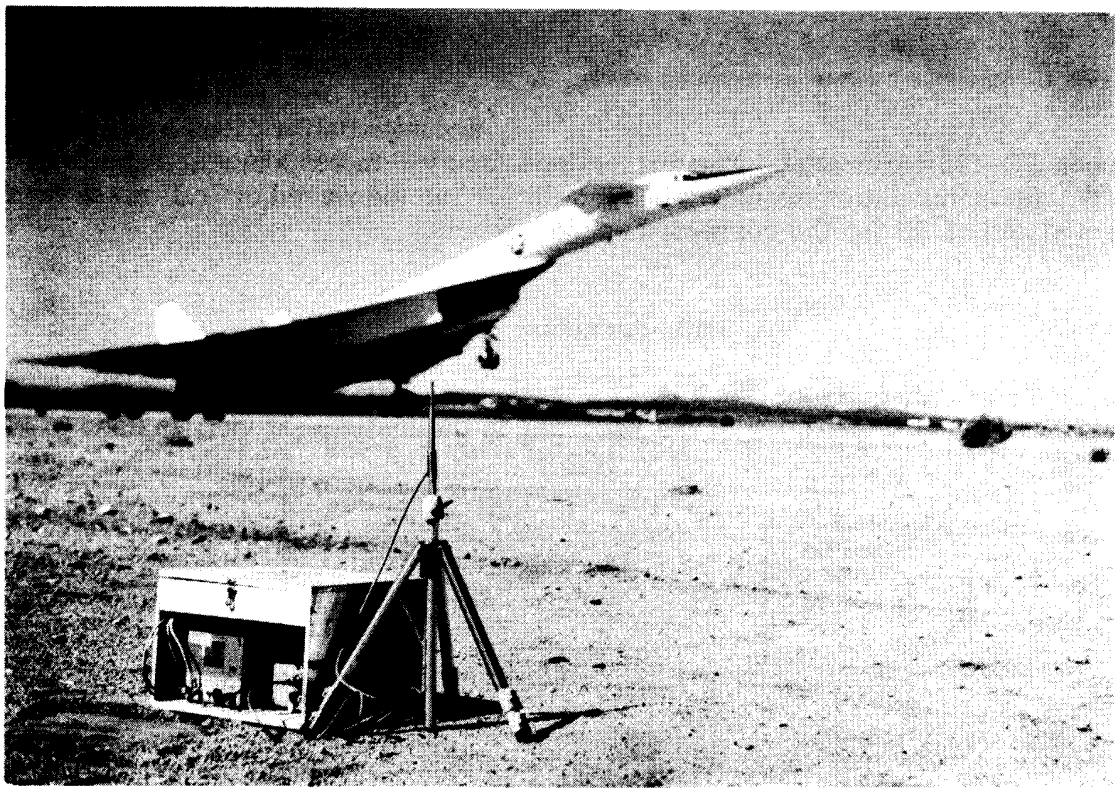

Figure 3.– Test airplane and a typical microphone station.

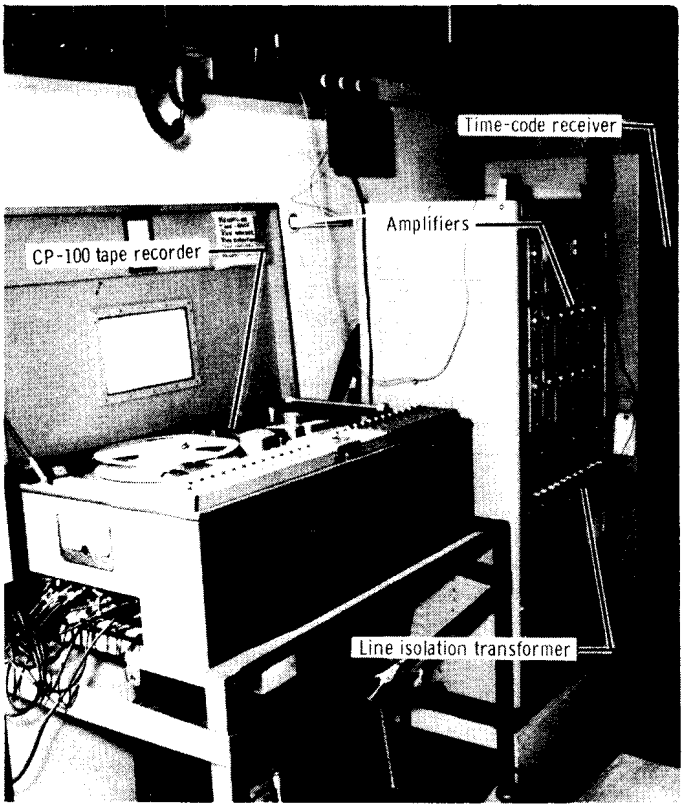

E-13137

Figure 4.— Signal conditioning and recording system.

A signal conditioning and recording system, shown in figure 4, is located in a van. The signal input from each microphone station is terminated at a line isolation transformer, routed to an amplifier, and then recorded on magnetic tape. Time of day from the time-code receiver is also recorded on the tape, thus providing a correlation with aircraft space positioning and airplane data.

The entire instrument range was calibrated electrically and acoustically. The electrical calibration consisted of introducing a 1-volt root-mean-square signal at various frequencies from 20 hertz to 20,000 hertz and determining any variation in recorded signal level. The microphone and electrical-system calibrations were combined to obtain the total recording-system calibration.

Periodic system recalibrations are performed to insure that the system response does not vary more than ±0.2 dB. Pre-test and post-test acoustic calibrations are made with a Photocon PC-125 calibrator. The corrections for system response are shown in table II. Instrumentation accuracy is ±1.5 dB for the measured overall noise levels presented and ±1 dB for the corrected spectra levels.

Data-Reduction System

A schematic diagram of the noise-analysis system is shown in figure 5. A tape recorder, which is a duplicate of the recorder in the instrument van, is used to recover

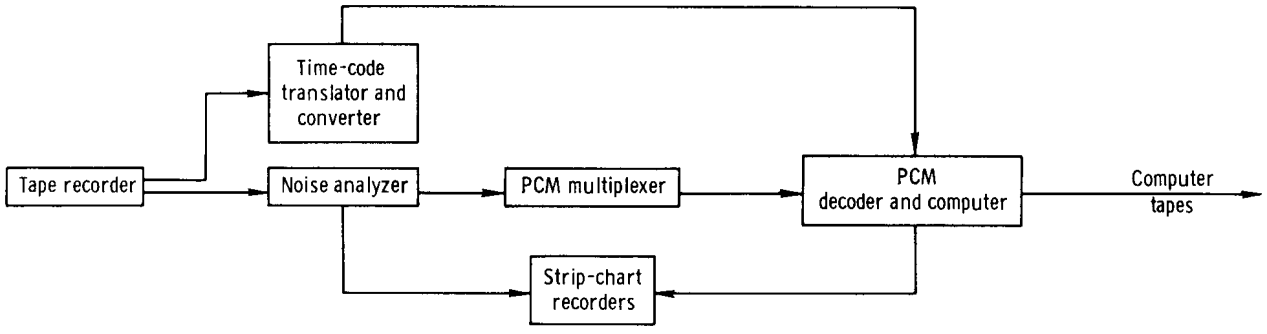

Figure 5.— Schematic diagram of the noise-analysis system.

the data signal, and the signal is then routed to a noise analyzer. Parallel outputs of either octave bands or one-third octave bands from the analyzer, along with a time signal, are fed to strip charts for analog readout. The parallel filter outputs are also fed to a pulse-code modulation multiplexer and then to a computer where the data are digitized on tape. The digital tape is formulated for further computer processing to obtain time-history tabulation of the octave or one-third octave band sound-pressure levels. Octave band levels were used for all data in this paper.

In addition, the actual energy acceptance of each filter was determined by using an electrical calibration. No corrections for the filter were necessary since the maximum effect of the filter on the data was ±0.14 dB. Periodically, the system is checked to insure that the filter effect remains small.

Space Positioning

Space positioning for all XB-70 operations in the vicinity of the runway is obtained from the Air Force Askania cinetheodolites (ref. 5) mounted in towers approximately 1 mile (1609 meters) north of the center of the runway and 1 mile (1609 meters) in from each end of the runway (fig. 1). Each camera frame shows the azimuth and elevation dial readings and a binary time-of-day code. All space-positioning data were corrected from the tracking reference on the XB-70 to the centerline and exhaust plane of the engines.

TEST AIRPLANE

The XB-70 (fig. 3) is a large supersonic airplane powered by six YJ93-GE-3 engines, which are afterburning turbojets installed side by side (fig. 6). Engine inlets consist of two large variable-throat ducts, each supplying air to three engines. The afterburner is a convergent-divergent type with a fully variable nozzle. Performance details are given in reference 6.

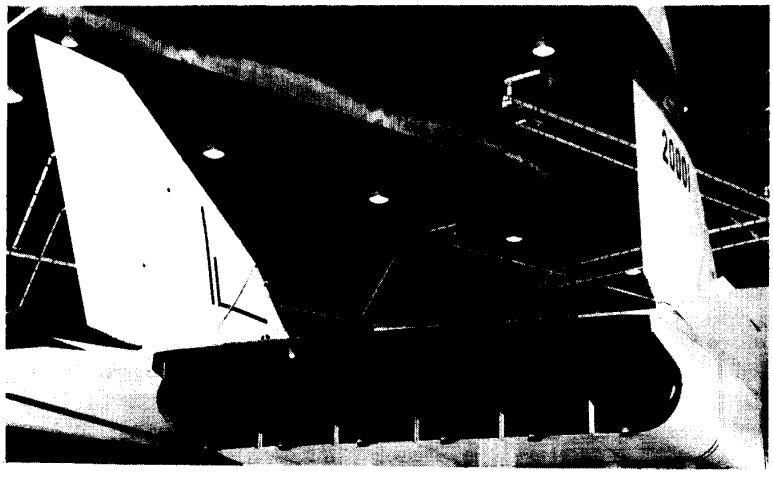

E-17193

Figure 6.– Photo showing engines installed in XB-70 airplane.

TESTS

All noise measurements were made during the Air Force XB-70 flight program. No noise-abatement procedures were used. The data presented are for three takeoffs, one landing, and one flyby. The data on weather conditions in table I were obtained from the Air Force.

Takeoff velocities and profiles for flights 1, 2, and 3[a] are shown in figure 7. The zero point represents brake release, which was approximately 350 feet (107 meters) from the end of the runway for each flight. Flights 1 and 2 were from west to east.

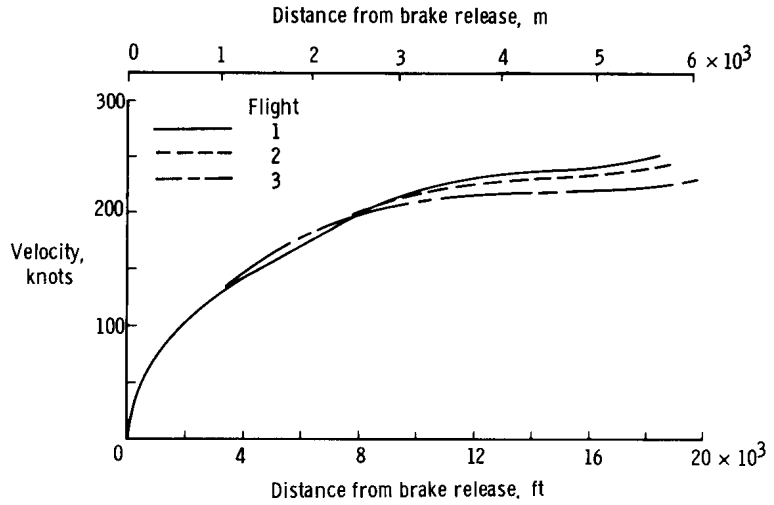

(a) Variation of velocity with distance from brake release.

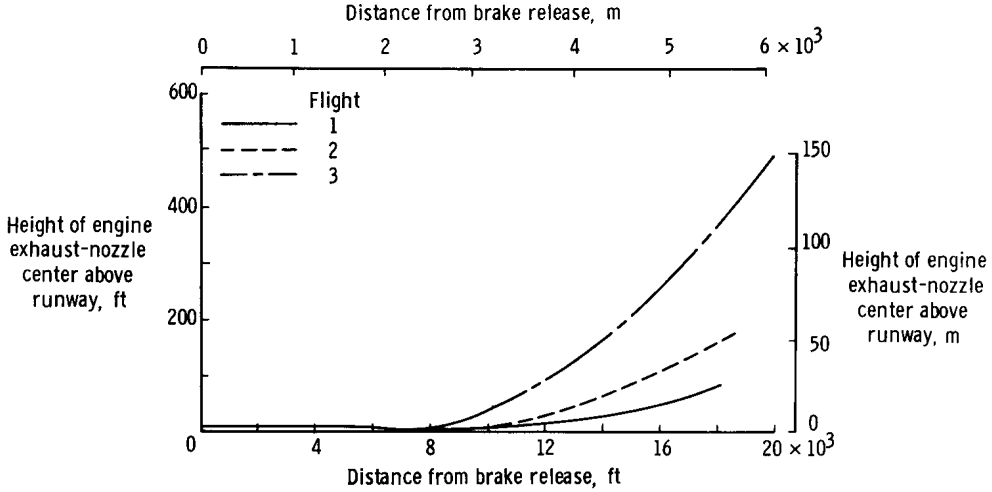

(b) Variation of altitude with distance from brake release.

Figure 7.— Takeoff profiles and velocities of the XB-70 on flights 1, 2, and 3 .

For flight 1 noise was measured on microphones 1, 3, 4, 5, and 6. Microphone 2 was inoperative. Data for flight 2 were obtained on microphones 3, 4, 5, and 6. Flight 3 was from east to west, and noise was measured on microphones 5, 7, 8, 9, and 10. Because of interference from aircraft ground support equipment, microphones near the XB-70 at brake release were not used. Profiles are given in terms of height of the

[a]Flight numbers herein do not correspond to flight numbers in the XB-70 program.

engine exhaust-nozzle center above the ground, since this is the noise source of interest. All noise data obtained during takeoff were with afterburner power settings. Airplane gross weight at each takeoff was approximately 500,000 pounds (227,000 kilograms).

The landing velocity and glide slope for flight 4 are shown in figure 8. The landing was from west to east, and data were obtained only on microphones 7, 9, and 10. All engines were at idle, and brake parachutes were deployed shortly after touchdown. The glide slope was less than 1°, as can be seen in the figure.

The flyby, flight 5, was from east to west, 80 feet (24 meters) above the runway. There was an acceleration at the start of the flyby, then a constant speed was maintained. The aircraft velocity was 296 knots over microphones 1 and 2 and 302 knots over microphones 3, 4. 5, and 6. Microphones 7 and 8 were overdriven because of an increase in the thrust, and there was no tracking beyond microphones 7 and 8.

All noise data obtained during landing and the flyby were without afterburner.

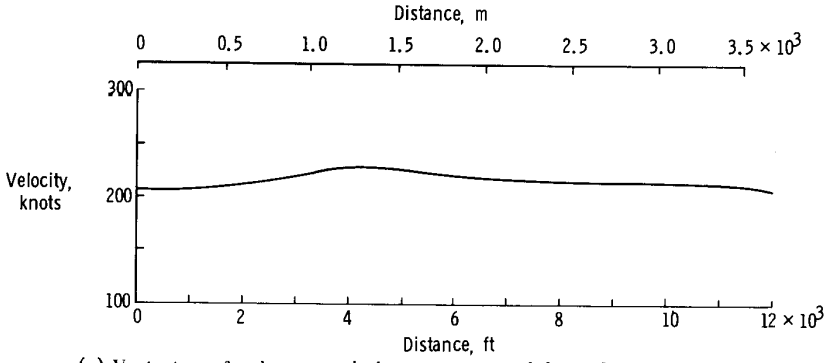

(a) Variation of velocity with distance to touchdown during approach.

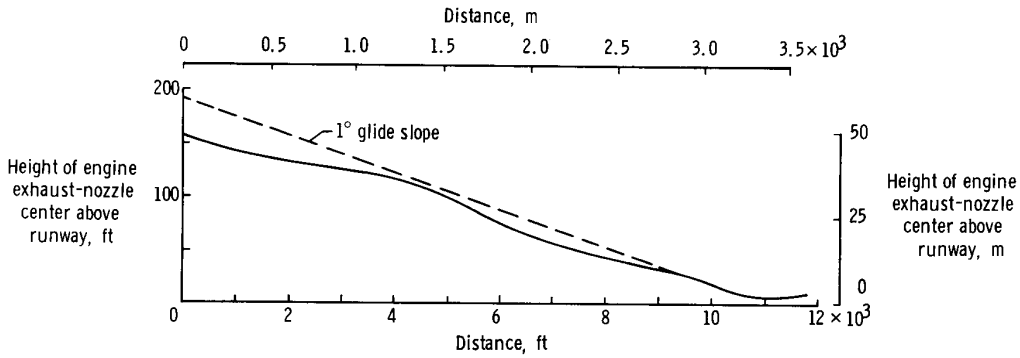

(b) Variation of altitude with distance to touchdown during approach.

Figure 8.– Landing velocity and profile of the XB-70 for flight 4.

RESULTS AND DISCUSSION

The summary of the XB-70 aircraft parameters in table III corresponds to the time that the maximum measured overall sound-pressure level was emitted from the engines.

Table IV is a summary of the pertinent geometric relationships, the measured and predicted maximum overall noise levels, and the computed and predicted perceived noise levels. The propagation distance in the table is the distance that the maximum measured overall sound-pressure level traveled from the aircraft to the microphone, as shown in figure 9.

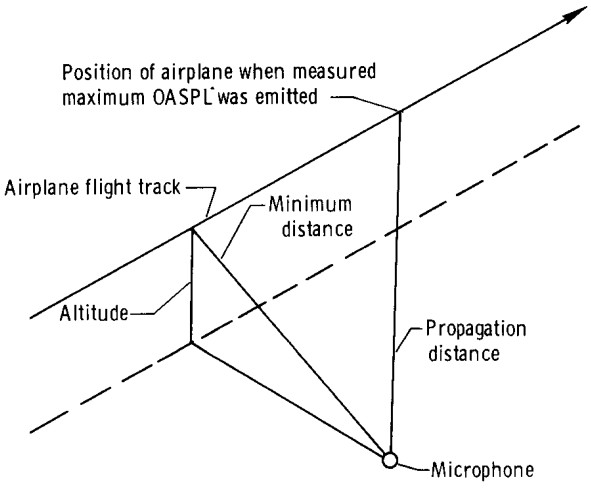

Figure 9.– Geometric relationship between the microphone and the aircraft.

Presented in figure 10 are comparisons of measured spectra with the theoretical spectra for a standard atmosphere, and the theoretical spectra for the actual atmosphere for two typical flights. The individual maximum sound-pressure levels of the octave bands and the overall sound-pressure levels occur within a time interval of less than 0.8 second. The predicted levels for the two highest octave bands when the actual atmosphere is used are low, whereas the standard-atmosphere results are in reasonable agreement with the measured spectra. The reason for this difference is unknown. Data presented in reference 7 showed that SAE atmospheric absorption values are too large above 2000 hertz. Standard atmosphere is used for all other predictions in this paper.

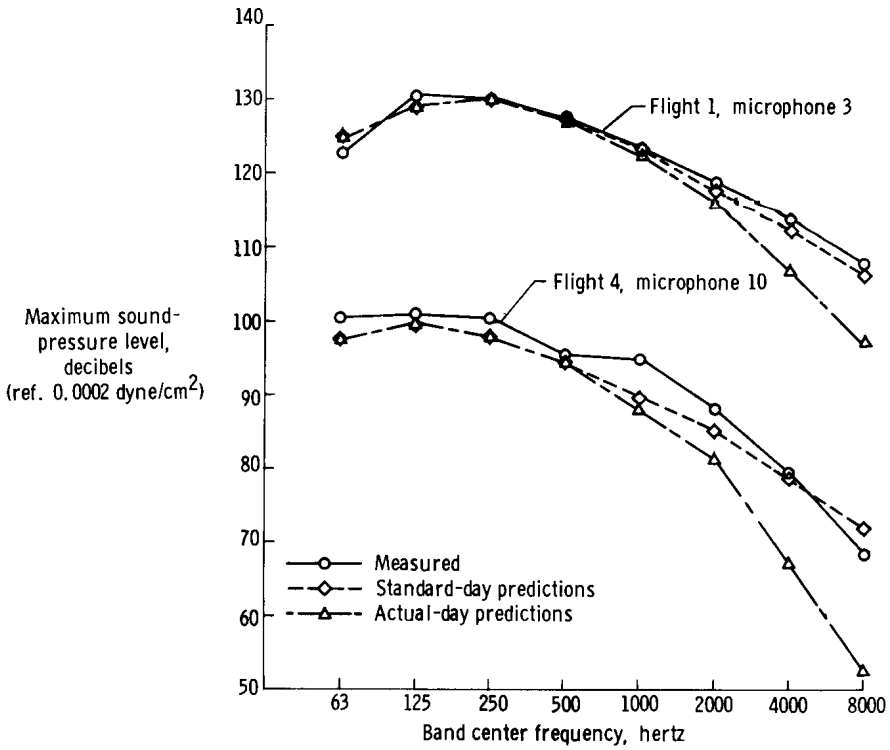

Figure 10.– Comparison of the measured spectra with the SAE standard-day predictions and the SAE actual-day predictions.

Comparisons of measured and predicted noise spectra at several microphone positions are shown in figures 11 to 15. The overall noise level and the octave-band spectra at each microphone are for the maximum levels recorded. All predictions were based on the engine parameters measured at the time the maximum noise originated from the engines. Askania cameras were not able to track in the vicinity of microphones 11 and 12; therefore, no noise data are presented for those microphone positions.

Presented in figures 11 to 13 are the measured and predicted noise spectra for the three takeoffs with engines operating at maximum afterburner. Both the in-flight and ground predictions are shown for the tests where the XB-70 had left the ground. In

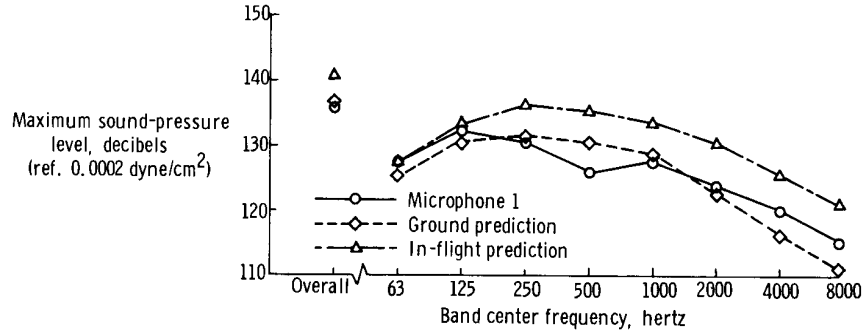

(a) Microphone 1.

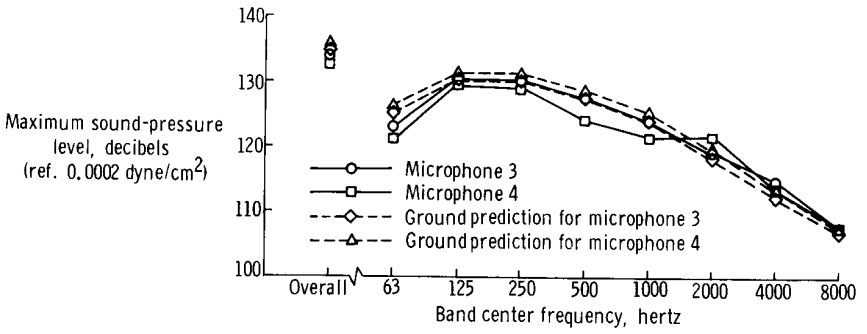

(b) Microphones 3 and 4.

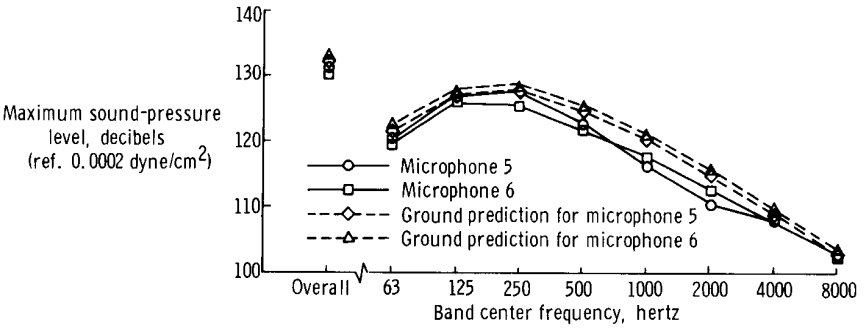

(c) Microphones 5 and 6.

Figure 11.– Frequency spectra and SAE predictions for flight 1 of the XB-70, a takeoff from west to east.

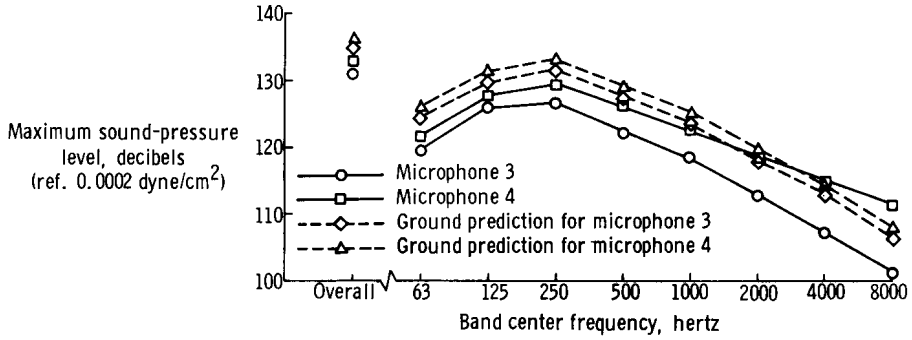

(a) Microphones 3 and 4.

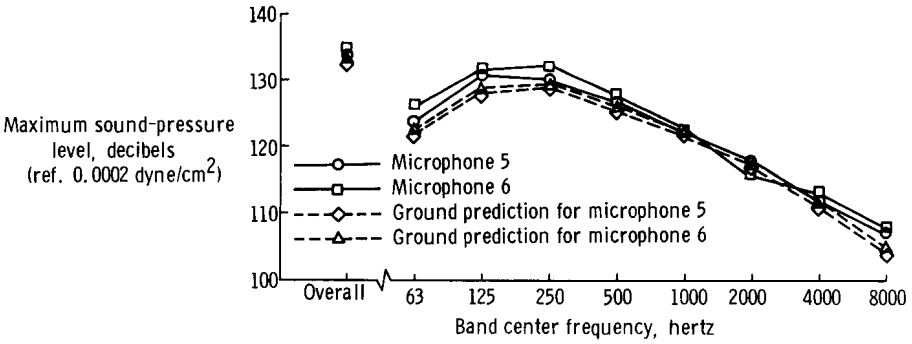

(b) Microphones 5 and 6.

Figure 12.– Frequency spectra and SAE predictions for flight 2 of the XB-70, a takeoff from west to east.

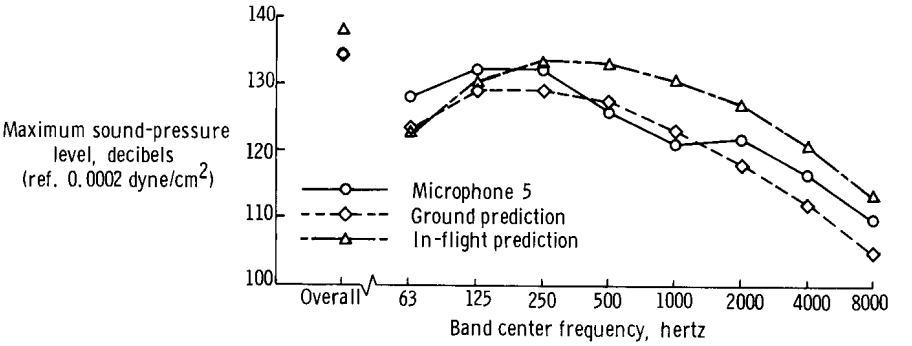

(a) Microphone 5.

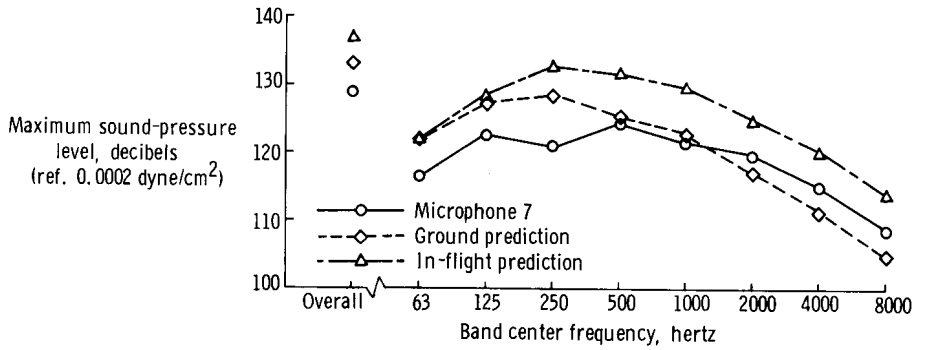

(b) Microphone 7.

Figure 13.– Frequency spectra and SAE predictions for flight 3 of the XB-70, a takeoff from east to west.

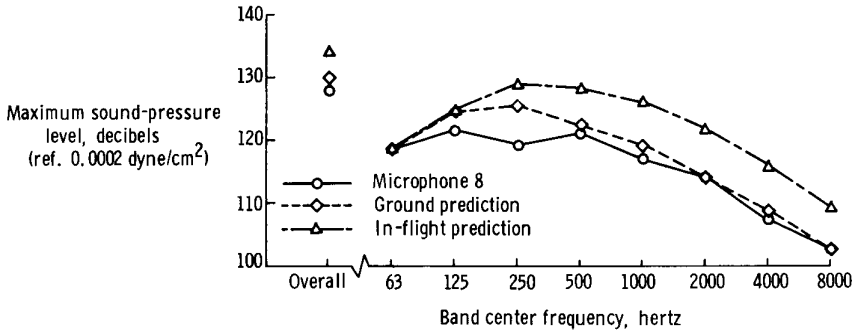

(c) Microphone 8.

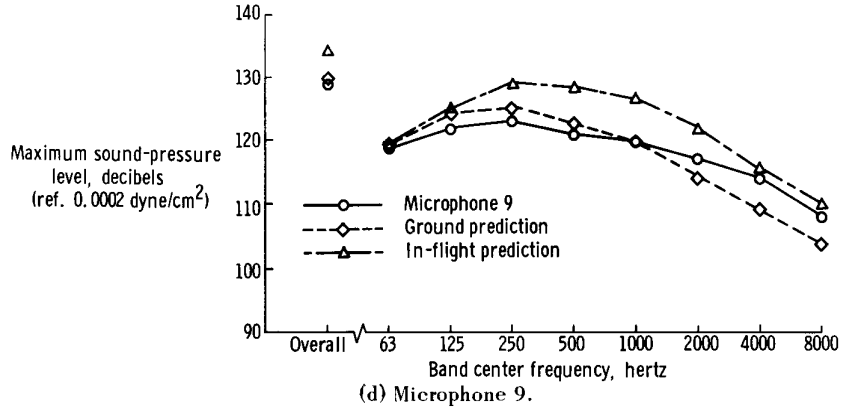

(d) Microphone 9.

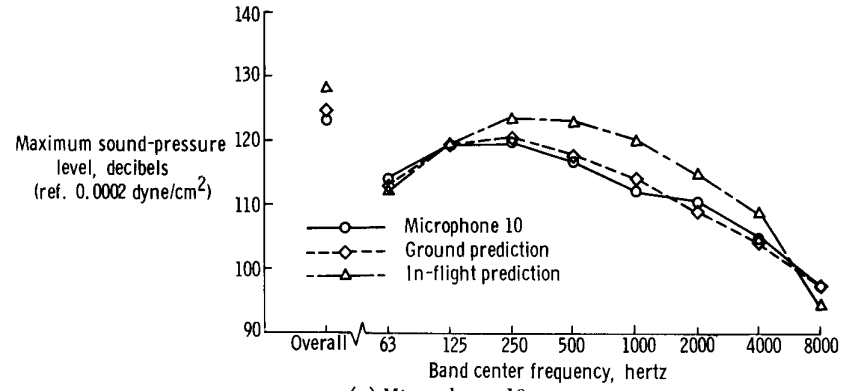

(e) Microphone 10.

Figure 13.– Concluded.

general, the levels predicted by using the ground prediction method showed more reasonable agreement with the measured octave band sound-pressure levels than did the levels predicted by the in-flight prediction methods. The measured maximums occurred in the 125 hertz and 250 hertz octave bands, and the octave band sound-pressure levels decreased with an increase in frequency. An unexplained exception was the frequency spectra obtained at microphones 7 and 8 for flight 3 (figs. 13(b) and 13(c)) where a peak occurred in the 500 hertz band. Overall sound-pressure levels up to 136 dB were measured during the takeoffs.

The noise spectra for the landing (fig. 14) were similar to those for the takeoffs, although the sound-pressure levels are approximately one order of magnitude lower.

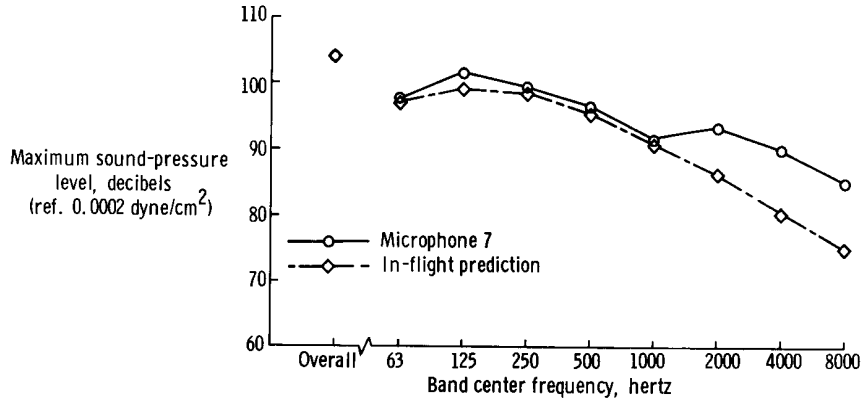

(a) Microphone 7.

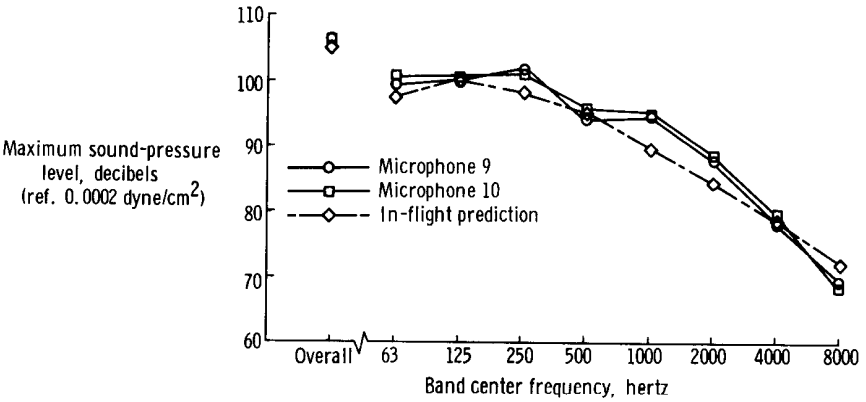

(b) Microphones 9 and 10.

Figure 14.– Frequency spectra and SAE prediction for flight 4 of the XB-70, a landing from west to east.

The measured and predicted noise spectra for the flyby are shown in figure 15. The flyby noise spectra differed from those of the takeoffs and landing in that the bands with center frequencies of 63, 125, and 250 hertz are 2 dB to 6 dB lower than predicted.

Presented in figure 16 are the maximum overall sound-pressure levels that were measured during takeoff and a theoretical inverse-square curve for the overall sound-pressure levels to be expected at the given distances. The curve is an inverse-square curve to indicate reduction of sound due to distance and does not include any atmospheric attenuation. Although the data are scattered about the theoretical curve, the agreement is reasonable and indicates little effect of atmospheric attenuation on the overall sound levels.

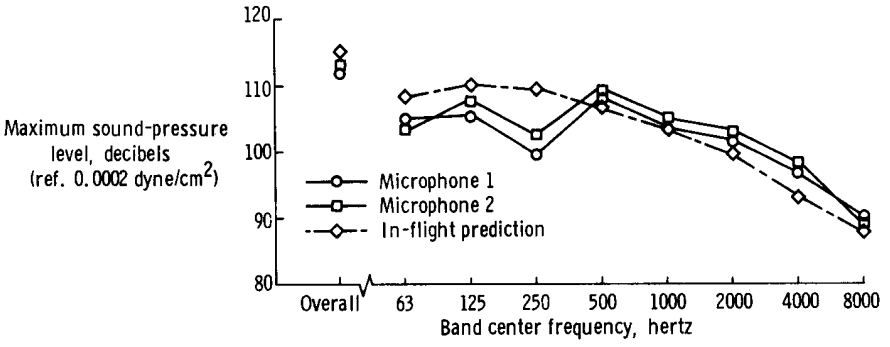

(a) Microphones 1 and 2.

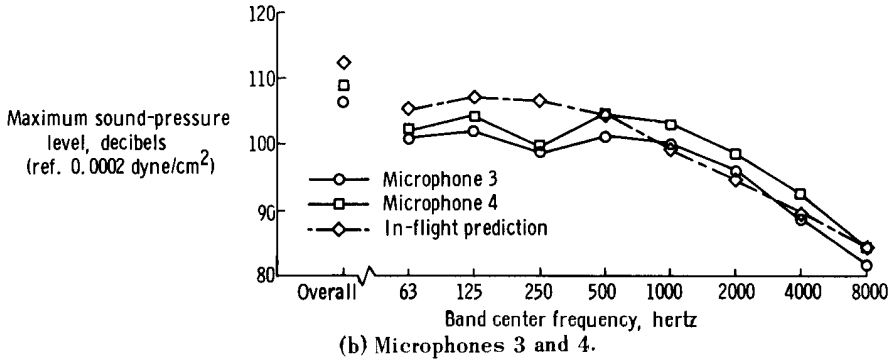

(b) Microphones 3 and 4.

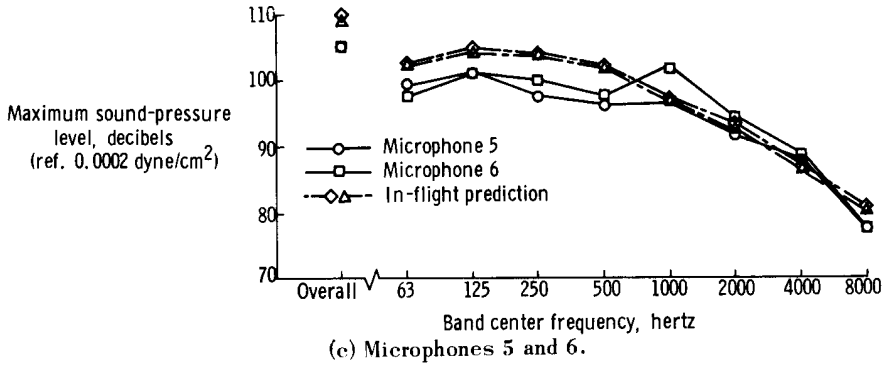

(c) Microphones 5 and 6.

Figure 15.– Frequency spectra and SAE predictions for flight 5 of the XB-70, a flyby at an engine height of 80 feet (24 meters) above the runway.

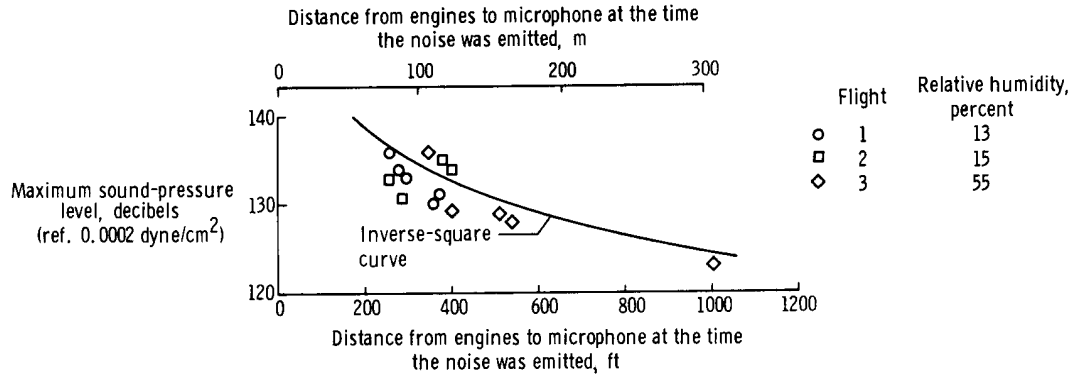

Figure 16.– Maximum overall sound-pressure levels measured during takeoff of the XB-70 with engines in maximum afterburner.

Figure 17 is a comparison of the maximum overall sound-pressure levels and the computed perceived noise levels of the XB-70 airplane for all tests. The perceived noise levels are approximately 7 PNdB to 10 PNdB higher than the maximum overall sound-pressure levels in decibels. The perceived noise levels were significantly higher in relation to the overall noise level in decibels when the airplane was not in afterburner power setting (landing and flyby).

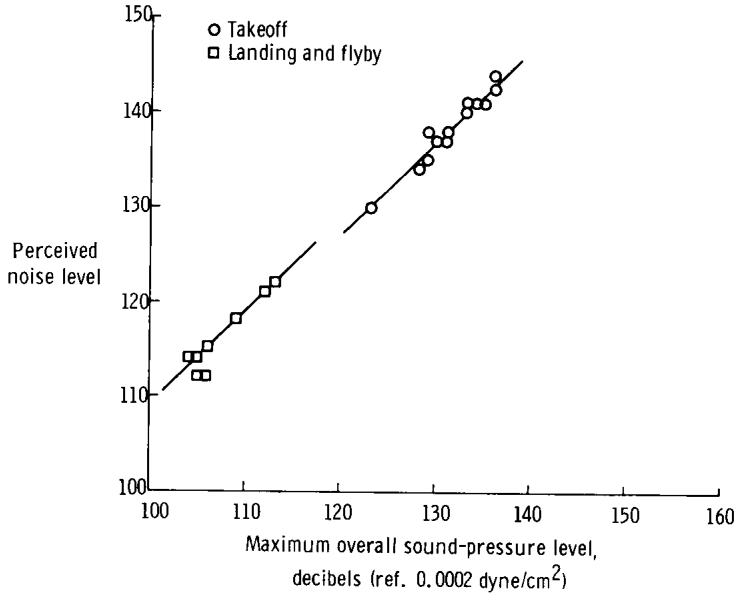

Figure 17.– Perceived noise levels of the XB-70.

CONCLUDING REMARKS

Measured data obtained during takeoff, landing, and flyby of the XB-70 were used to determine the applicability of the SAE prediction method to the XB-70 airplane. There were significant differences between the measured and the predicted noise levels when actual atmospheric conditions were used. By using standard-day atmosphere for the predictions, reasonable agreement was obtained with measured data. More data are needed to determine the reasons for the differences in measured and predicted noise levels. Perceived noise levels of the XB-70 were approximately 7 PNdB to 10 PNdB higher than the maximum overall sound-pressure levels in decibels.

Flight Research Center,
National Aeronautics and Space Administration,
Edwards, Calif., September 27, 1967,
126-16-03-01-24.

APPENDIX

ANALYSIS OF ERRORS CAUSED BY ENGINE PARAMETERS

The SAE jet-noise prediction method (ref. 2) is based on the relationship for overall sound-pressure level:

$$\text{OASPL} = 10 \log f(V_R) + 10 \log \rho^2 A \tag{1}$$

where ρ is the weight density of the fully expanded jet, A is the cross-sectional area of the jet exhaust at the nozzle exit, and 10 log $f(V_R)$ is an empirically determined relationship between jet noise and the velocity of jet exhaust relative to ambient air V_R, as shown in figure 18.

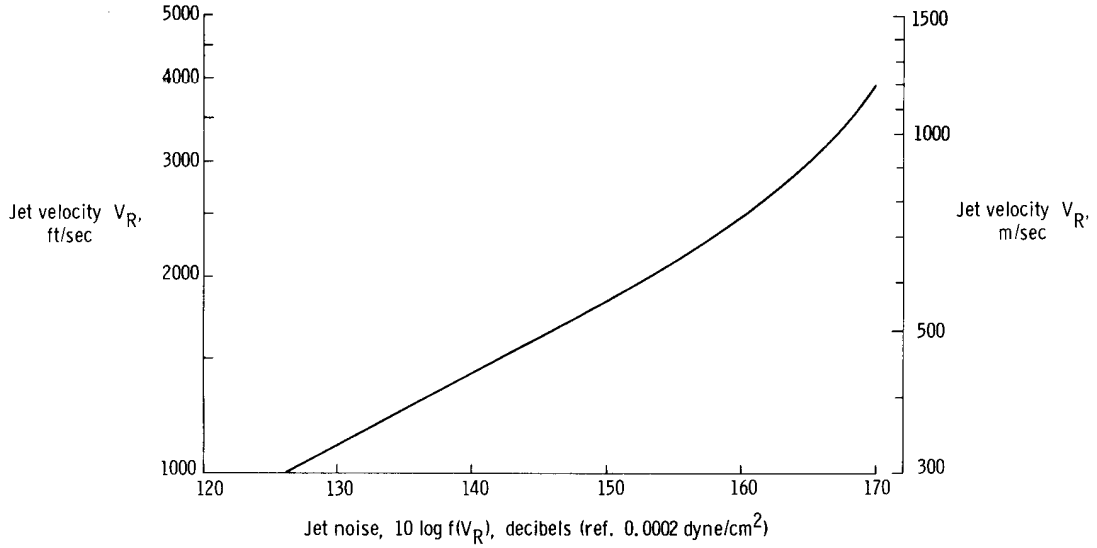

Figure 18.– Normalized jet noise as a function of jet relative velocity. Normalized for ρ=1 lb/ft^3(16.0 kg/m^3) and A=1 ft^2(.0929 m^2). Adapted from reference 2.

The equation

$$10 \log f(V_R) \approx 93.5 \log V_R + B \tag{2}$$

where B is a constant, defines the curve in the figure when $V_R \leqq 2100$ ft/sec (640 m/sec). From equations (1) and (2)

$$\text{OASPL} = 10 \log \rho^2 A + 93.5 \log V_R + B \tag{3}$$

Substituting

$$V_R = \frac{gF_N}{W} \tag{4}$$

and

$$\rho = \frac{W}{AV_j} \tag{5}$$

where g is the acceleration due to gravity, F_N is the net thrust, W is the weight flow of exhaust gas, and V_j is the velocity of jet exhaust relative to the nozzle, into equation (3)

$$\text{OASPL} = 10 \log \frac{W^2}{AV_j^2} + 93.5 \log \frac{gF_N}{W} + B \tag{6}$$

and differentiating

$$d(\text{OASPL}) = 8.7\frac{dW}{W} - 4.3\frac{dA}{A} - 8.7\frac{dV_j}{V_j} + 40.6\frac{dF_N}{F_N} - 40.6\frac{dW}{W} \tag{7}$$

Since the maximum possible value of error is desired, all negative signs will be treated as additive. Rewriting equation (7)

$$d(\text{OASPL}) = 49.3\frac{dW}{W} + 40.6\frac{dF_N}{F_N} + 8.7\frac{dV_j}{V_j} + 4.3\frac{dA}{A} \tag{8}$$

Based on the curve in figure 18, equation (8) shows the error in decibels due to inaccurate measurements of W, F_N, V_j, and A. When $V_R > 2100$ ft/sec (640 m/sec),

$$10 \log f(V_R) < 93.5 \log V_R + B \tag{9}$$

and it can be shown in a similar manner that

$$d(\text{OASPL}) \leqq 49.3\frac{dW}{W} + 40.6\frac{dF_N}{F_N} + 8.7\frac{dV_j}{V_i} + 4.3\frac{dA}{A} \tag{10}$$

REFERENCES

1. Anon.: Definitions and Procedures for Computing the Perceived Noise Level of Aircraft Noise. ARP 865, SAE, Oct. 15, 1964.

2. Anon.: Jet Noise Prediction. AIR 876, SAE, July 10, 1965.

3. Anon.: Standard Values of Atmospheric Absorption as a Function of Temperature and Humidity for Use in Evaluating Aircraft Flyover Noise. ARP 866, SAE, Aug. 31, 1964.

4. Tanner, Carole S.; and McLeod, Norman J.: Preliminary Measurements of Take-off and Landing Noise From a New Instrumented Range. Conference on Aircraft Operating Problems, NASA SP-83, 1965, pp. 83-90.

5. Taylor, Albert E.: Evaluation of Take-off and Landing Facility. Tech. Memo. FTFF-TM-58-12, U.S. Air Force Flight Test Center, Apr. 1958.

6. Wolfe, J. E.: Propulsion System Performance Substantiation Report for the XB-70A Air Vehicle (YJ93-GE-3 Engines). Rep. NA-64-674, North American Aviation, Inc. (Contract AF33(600)-42058).

7. Franken, Peter A.; and Bishop, Dwight E.: The Propagation of Sound From Airport Ground Operations. Rep. 1389, Bolt Beranek and Newman Inc. (Van Nuys, Calif.), Jan. 4, 1967.

TABLE I. – WEATHER CONDITIONS DURING THE NOISE TESTS

Flight	Atmospheric pressure,		Temperature,		Percent relative humidity	Wind velocity, knots	Wind direction[1], deg
	lb/ft^2	N/m^2	° F	° K			
1	1944	93,080	85	302	13	3	170
2	1953	93,510	72	295	15	2	190
3	1937	92,740	59	288	55	10	260
4	1947	93,220	90	305	11	3	171
5	1953	93,510	66	292	46	8	238

[1]Direction from which wind was blowing.

TABLE II. – TOTAL SYSTEM CORRECTIONS FOR EACH MICROPHONE STATION

Band center frequency, hertz	Corrections for microphone stations, dB (ref. 0.0002 $dyne/cm^2$)											
	1	2	3	4	5	6	7	8	9	10	11	12
63	-1.6	-1.8	-1.9	-0.7	-0.9	-0.7	-0.6	-0.9	-0.7	-0.8	-1.2	-0.8
125	-1.1	-.3	-.4	-.4	0	-.4	-.3	-.5	-.3	-.4	-.2	-.4
250	-.1	0	0	.1	-.1	-.1	0	-.1	0	-.1	-.1	0
500	0	0	0	0	-.1	0	0	0	0	-.1	-.1	0
1000	0	0	0	0	0	0	0	0	0	0	0	0
2000	.2	0	0	.1	0	-.1	.1	0	0	0	-.1	0
4000	.2	-.3	-.4	-.4	-.2	-.2	-.1	-.3	-.2	-.4	-.2	-.4
8000	-.3	-1.0	-1.2	-1.0	-.8	-.6	-.4	-.3	-.9	-1.6	-.8	-1.0

TABLE III. – SUMMARY OF XB-70 OPERATING PARAMETERS

Flight	Profile	Microphone station	Gross weight,		Ground speed,	Velocity of jet V_R,		Exit nozzle area,		Weight flow of exhaust,		Weight density of expanded jet,	
			lb	kg	knots	ft/sec	m/sec	ft^2	m^2	lb/sec	kg/sec	lb/ft^3	kg/m^3
1	Takeoff	1	500,000	227,000	236	2860	872	8.78	0.816	264	120	9.23×10^3	0.148
1	Takeoff	3	500,000	227,000	219	2850	869	8.81	.818	255	116	8.98	.144
1	Takeoff	4	500,000	227,000	219	2850	869	8.81	.818	255	116	8.98	.144
1	Takeoff	5	500,000	227,000	160	2780	847	8.82	.819	248	112	9.22	.148
1	Takeoff	6	500,000	227,000	160	2780	847	8.82	.819	248	112	9.25	.148
2	Takeoff	3	508,000	230,000	219	2740	835	8.85	.822	294	133	10.7	.171
2	Takeoff	4	508,000	230,000	219	2740	835	8.85	.822	294	133	10.7	.171
2	Takeoff	5	508,000	230,000	162	2840	866	8.85	.822	269	122	9.47	.152
2	Takeoff	6	508,000	230,000	162	2840	866	8.85	.822	269	122	9.47	.152
3	Takeoff	5	513,000	233,000	208	3020	920	8.71	.809	285	129	9.70	.155
3	Takeoff	7	513,000	233,000	224	3080	939	8.71	.809	285	129	9.47	.152
3	Takeoff	8	513,000	233,000	224	3080	939	8.71	.809	285	129	9.47	.152
3	Takeoff	9	513,000	233,000	232	3080	939	8.71	.809	285	129	9.40	.151
3	Takeoff	10	513,000	233,000	232	3080	939	8.71	.809	285	129	9.40	.151
4	Landing	7	285,000	129,000	205	1090	332	7.26	.674	180	81.6	17.3	.277
4	Landing	9	285,000	129,000	208	1090	332	7.37	.685	196	88.9	18.1	.290
4	Landing	10	285,000	129,000	208	1090	332	7.37	.685	196	88.9	18.1	.290
5	Flyby	1	342,000	155,000	296	1190	363	7.15	.664	210	95.3	17.5	.280
5	Flyby	2	342,000	155,000	296	1190	363	7.15	.664	210	95.3	17.5	.280
5	Flyby	3	342,000	155,000	302	1170	357	7.18	.667	210	95.3	17.4	.279
5	Flyby	4	342,000	155.000	302	1170	357	7.18	.667	210	95.3	17.4	.279
5	Flyby	5	342,000	155,000	302	1180	360	7.14	.663	208	94.3	17.3	.277
5	Flyby	6	342,000	155,000	302	1180	360	7.14	.663	208	94.3	17.3	.277

TABLE IV. – SUMMARY OF XB-70 NOISE DATA

Flight	Profile	Microphone station	Engine height,		Minimum distance,		Propagation distance,		Maximum OASPL, dB	Maximum PNdB	SAE OASPL, dB	Predicted PNdB
			ft	m	ft	m	ft	m				
1	Takeoff	1	39	12	176	54	259	79	136	144	137	143
1	Takeoff	3	6	2	223	68	275	84	134	141	135	140
1	Takeoff	4	6	2	219	67	295	90	133	141	136	141
1	Takeoff	5	10	3	300	91	383	117	131	137	132	138
1	Takeoff	6	10	3	283	86	353	108	130	137	133	138
2	Takeoff	3	6	2	239	73	284	87	131	138	135	141
2	Takeoff	4	6	2	202	62	259	79	133	140	136	142
2	Takeoff	5	10	3	310	94	400	122	134	141	132	138
2	Takeoff	6	10	3	270	82	375	114	135	141	133	139
3	Takeoff	5	39	12	305	93	341	104	136	143	135	141
3	Takeoff	7	214	65	340	104	400	122	129	138	133	140
3	Takeoff	8	215	66	485	148	540	165	128	134	130	136
3	Takeoff	9	505	154	495	151	550	168	129	135	130	136
3	Takeoff	10	535	163	920	280	1010	308	123	130	125	131
4	Landing	7	30	9	361	110	401	122	104	114	104	109
4	Landing	9	110	34	440	134	488	149	106	112	104	111
4	Landing	10	110	34	445	136	495	151	106	112	104	111
5	Flyby	1	80	24	168	51	235	72	112	121	115	121
5	Flyby	2	80	24	170	52	238	73	113	122	115	121
5	Flyby	3	80	24	233	71	260	79	106	115	112	117
5	Flyby	4	80	24	234	71	260	79	109	118	112	117
5	Flyby	5	80	24	283	86	396	121	105	112	111	116
5	Flyby	6	80	24	317	97	443	135	105	114	110	115